Electrical Power and Energy Systems 141 (2022) 108099

Contents lists available at ScienceDirect

International Journal of Electrical Power and Energy Systems

journal homepage: www.elsevier.com/locate/ijepes

An intelligent adaptive control of DC–DC power buck converters

Hoda Sorouri [a], Mostafa Sedighizadeh [a,*], Arman Oshnoei [a], Rahmat Khezri [b]

[a] Faculty of Electrical and Computer Engineering, Shahid Beheshti University, Tehran, Iran
[b] College of Science and Engineering, Flinders University, Adelaide, Australia

ARTICLE INFO

Keywords:
Buck DC–DC converters
Artificial neural network
Disturbance observer
Backstepping controller

ABSTRACT

Buck DC–DC converters are broadly used in DC microgrids to provide a constant dc voltage for generation and storage components. Changing of load condition affects the quality of voltage in the buck DC–DC converters. When constant power loads (CPLs) are used, the stability of these power electronic devices is at risk due to negative impedance characteristics of the CPLs. In such condition, an efficient control method is required to ensure the proper operation of the converter. For this purpose, development of an adaptive control methodology is essential to evaluate the accurate values of controller parameters in the shortest time to damp the ripples quickly. This paper develops a backstepping controller with nonlinear disturbance observer to regulate the output voltage of a dc/dc converter feeding a CPL. An artificial neural network (ANN) methodology is used to estimate the backstepping control parameters of the buck converter. The training ability of the ANN technique prevents the existing controller from depending on the working point of the microgrid. The ANN methodology adapts the controller with various changes and reflections of uncertainties in the microgrid. Case studies are conducted on a dc/dc buck converter in MATLAB/Simulink environment, and the results are verified by the OPAL-RT real-time simulator.

1. Introduction

Recently, DC systems are broadly used in transportation systems, microgrids, power systems, etc. [1–3]. The DC microgrids are based on power electronic devices which add several advantages like low weight and volume, high efficiency and flexibility, as well as isolation, controllability, etc. [4,5]. Switching dynamics of the dc/dc converter lead the DC microgrids to a nonlinear behavior. Hence, adjusting the output voltage is a challenging task [6]. Attaining an appropriate control method for dc/dc converters is an important task to better understand the design aspect of the controller and stability problem [7,8]. In addition, it is helpful to improve transient and steady-state conditions in various perturbations.

Power electronic converter loads, when they are fully controlled, act like constant power loads (CPLs). CPLs have negative impedance which may cause instability in the DC bus and thus the entire microgrid [1,4,9]. This means that CPLs may affect the electrical quality of the microgrid and cause instability, which may eventually lead the system operation to fail [10,11]. Classic linear controllers are generally used in dc/dc converter controllers. Small signal models are also used to analyze the stability of controllers and in the design stage of dc/dc converter feeding CPLs, where the system equations are linearized around an equilibrium point and then they are analyzed using classical eigenvalue or frequency domain [12]. However, because of the nonlinear feature of the systems, linear control techniques may only guarantee small signal stability. However, in large disturbances, they are not effective for load changes. Recently, the large signal analysis methods like Lyapunov analysis have been used to analyze the stability of dc–dc converters in disturbances [13]. In [14], the controller is created by passive elements to regulate the voltage of a DC microgrid with CPLs. This approach is made for a specific MG with complete and accurate knowledge about the system parameters. Design of filter parameters is locally implemented. For example, an electromagnetic interference filter may only be designed based on its frequency response. However, these filters as well as CPLs have great impacts on the stability and robustness of the DC microgrids. A smaller capacitor connected to the CPL reduces the stability boundary and a larger capacitor increases the size and cost [15]. In fact, passive damping strategies like using capacitors and resistors [16], or filters [17] are simple and useful, while the cost and physical limitations are the restrictions. In [18], a linearized control strategy is suggested for the buck converter with CPL. This method improves the transient response if the load is disturbed, while converters are nonlinear. Due to the negative impedance of the CPLs, nonlinear controllers must be used to achieve a stable system. In [19], a model predictive control (MPC) method is proposed to

* Corresponding author.
E-mail address: M_Sedighi@sbu.ac.ir (M. Sedighizadeh).

https://doi.org/10.1016/j.ijepes.2022.108099
Received 16 July 2021; Received in revised form 4 December 2021; Accepted 25 February 2022
Available online 29 March 2022

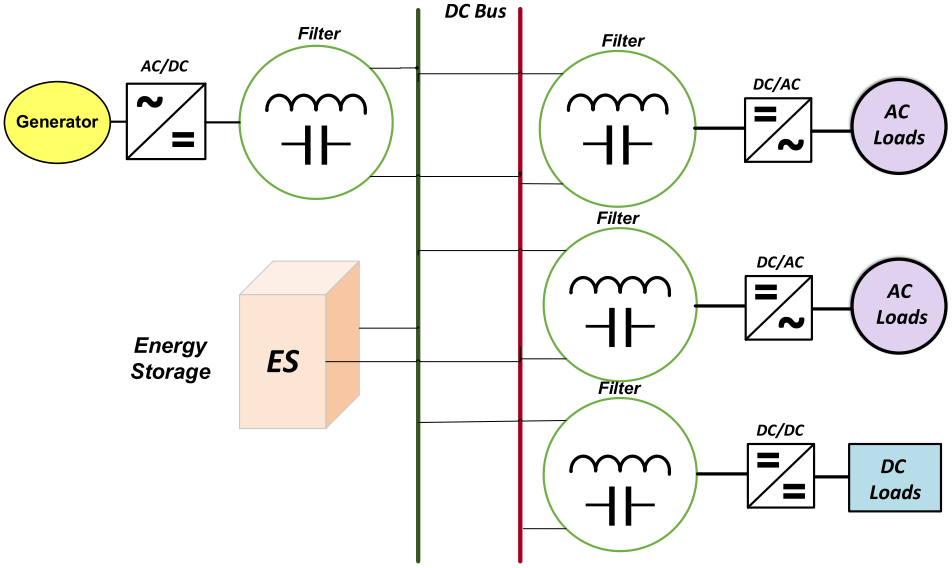

Fig. 1. A simplified schematic diagram of a DC microgrid.

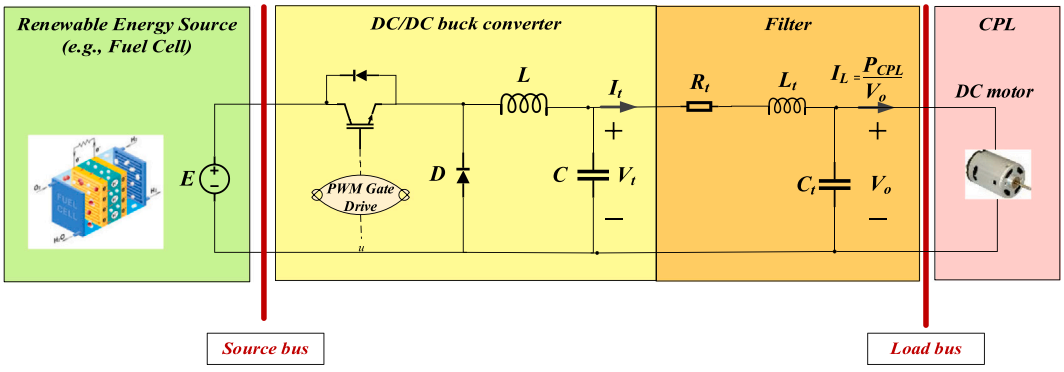

Fig. 2. Circuit diagram of a renewable source with DC buck converter.

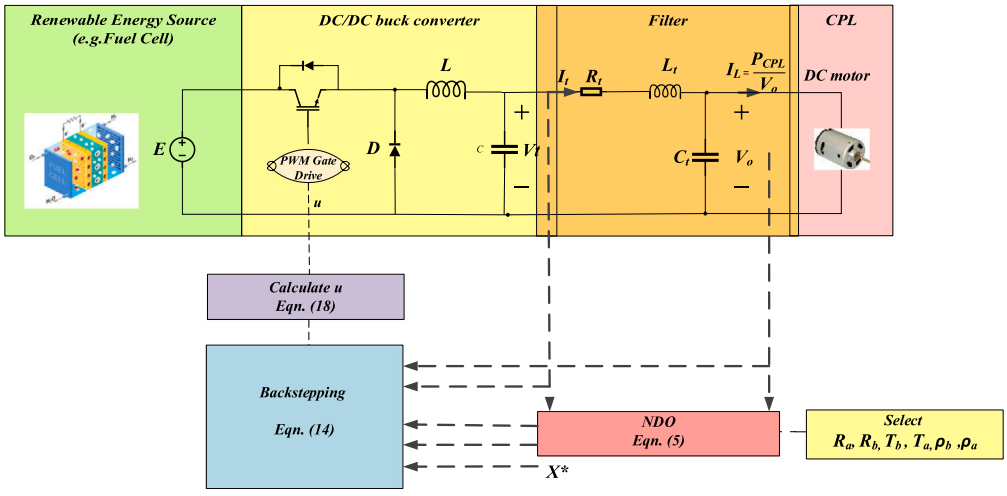

Fig. 3. Converter control by the backstepping controller with observer.

control the boost converter with CPL. However, the online computational problem of MPC prevents its practical implementation. Slide mode control (SMC) is one of the nonlinear methods that has simple structure and is known for its strong robustness [20]. In [21], a new controller based on fractional-order sliding mode control is proposed for high-order nonlinear disturbances in a buck converter. Another sliding based control, known as second-order sliding mode approach, is designed for a neutral-point-clamped power converter in [22]. A

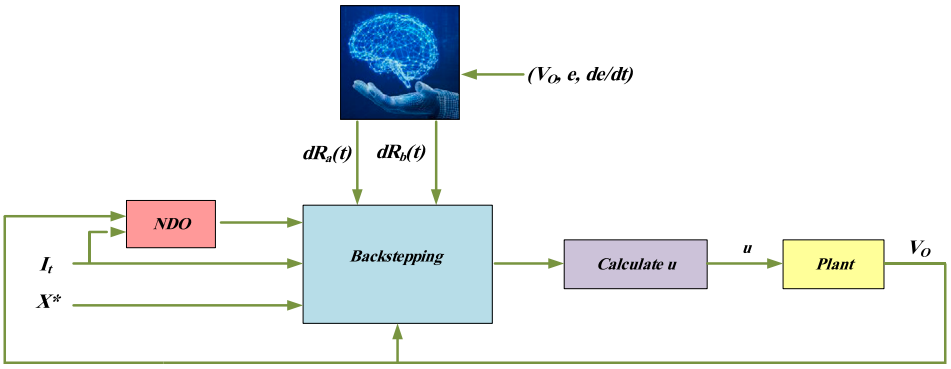

Fig. 4. Schematic of the proposed ANN supervisory control.

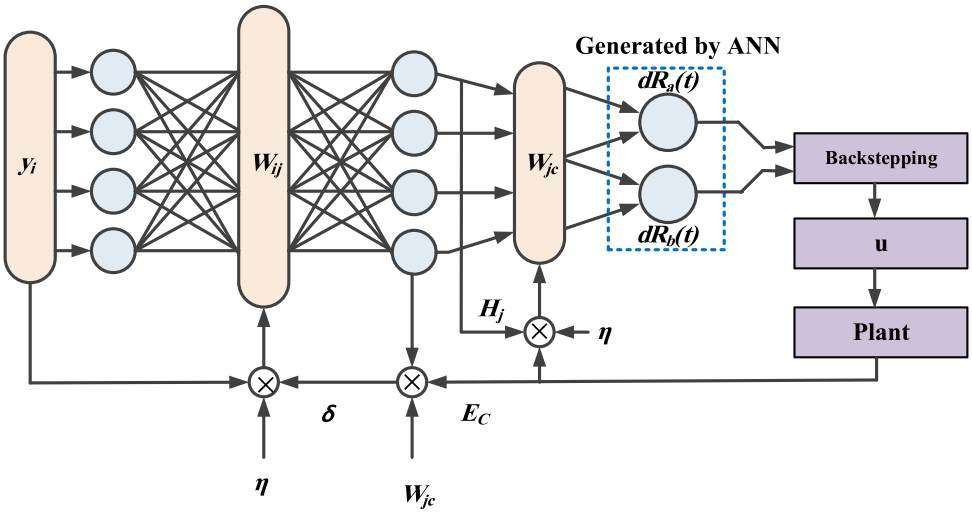

Fig. 5. Structure of the ANN to estimate the backstepping parameters.

high-order sliding mode control is proposed for an AC/DC converter in [23]. In [24], a three-layer controller is developed based on observer strategy and sliding mode control for a neutral-point-clamped converter. Nevertheless, the need for variable frequency switching leads to chattering problems. To measure the output current of the capacitor, a series of current sensors are needed that causes a higher equivalent series resistance. This reduces the effect of ripple filter and increases the output impedance.

Backstepping control is an important nonlinear control technique that can be used for DC microgrids in the form of accurate feedback [25, 26]. The main advantages of backstepping controller are systematic frame for controller design, easy to understand, simple performance, linear parameter inconsistencies, nonconformities, and successful rule out for uncertainty. Adaptive backstepping control is one of the most effective nonlinear control methods for solving stability and tracking problems [27]. This method has been used for power electronic converter systems in [28–30]. The nonlinear disturbance observer (NDO) is a useful method for estimating online uncertainty/turbulence in nonlinear systems with minimal data of power system [31,32]. The NDO supplies a hopeful way for perturb and uncertainty compensation, which is a crucial aim in the design stage of a controller [33]. This method has received high attention because of providing a favorable solution for disorder and uncertainty problems [33]. In [34,35], adaptive backstepping control and NDO are used for estimation of uncertain changes in constant power load in a fast dynamic response which resulted in a fast and precise voltage tracking under high load changes.

This work proposes a novel backstepping controller with NDO for a buck dc/dc converter. A two-layer artificial neural network (ANN) with a recursive control technique is added to estimate the backstepping parameters to control a CPL. The behavior of backstepping control is improved using an ANN-based approximation method for the constant value of backstepping control with NDO. It is found that the speed of adaptation of the unknown parameter increases. The main contributions of this paper are as follows:

I. The voltage value of a dc/dc buck converter is adjusted by an adaptive backstepping control method with a NDO to improve the precise voltage tracking of the converter. The NDO has been used to estimate the variation of uncertainty in a fast dynamic response.
II. To improve the voltage and transient tracking accuracy of the converter, the voltage duration of the backstepping controller is adjusted and stabilized by the neural network. For this purpose, the gains of the backstepping controller are updated in an online manner to compensate the nonlinear observer estimation errors consistently.
III. The nonlinear reverse voltage caused by the CPLs imposes an instability to the DC power electronic converters, leading to significant fluctuations in the voltage or even a voltage collapse. The CPL's menace for stability intensifies when the reference voltage in the simulation is varied. In this paper, the effect of voltage reference changes on the buck converter supplying a CPL is studied to discuss the worst-case scenario for DC microgrids in terms of stability.
IV. The proposed control scheme is implemented in the real-time simulator, OPAL-RT-OP5600 to verify its applicability and effectiveness in real-time.

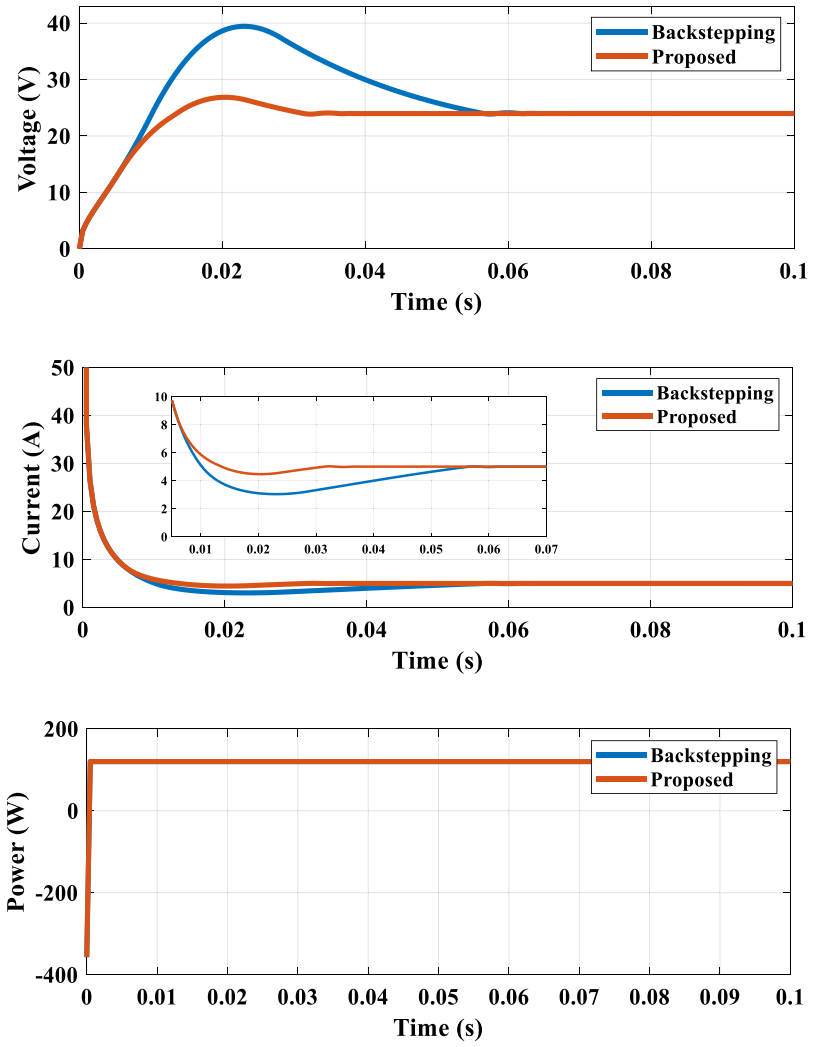

Fig. 6. The Simulation results in start-up in study 1.

This paper is organized as follows: Section 2 explains the system model with a CPL. In Section 3, the stability issue is described and a nonlinear observer is used to boost the performance of backstepping controller. The ANN is then proposed to estimate the parameters of the controller. Simulation verification in order to display the capabilities of the proposed method is indicated in Section 4. Finally, Section 5 concludes this paper.

2. Model of a DC/DC buck converter with CPL

A typical DC microgrid can be seen in Fig. 1 [3]. The dc/dc source converters supply the main dc bus. As seen, there are several dc/dc converters and the inverters are used to supply the AC loads presented in the scheme. In the case of supplying a resistive load with a dc/dc converter, the output power of the converter is constant and the output voltage of the converter is fully adjustable. For an inverter-motor drive system, when the motor speed is fully controlled by making the torque constant for one operating period, the output and input power of the inverter are constant. These fully controlled converter loads are known as constant power loads. Fig. 2 demonstrates a typical dc circuit diagram of a renewable source with a dc/dc buck converter supplying a CPL.

The dc/dc converters are adjusted by the u duty ratio of an IGBT switching to keep the output voltage stable. There is an input voltage source for the buck converter to supply the DC power. Given the fact that the CPL defines the load disturbances, it refers to a worst situation in the stability domain. The dynamic model can be represented by [36]:

$$\begin{aligned} \frac{dV_o}{dt} &= \frac{1}{C_t} I_t - \frac{1}{C_t} I_L \\ \frac{dI_t}{dt} &= -\frac{R_t}{L_t} I_t \end{aligned} \tag{1}$$

where I_t and I_L represent the currents of the converter and load, respectively; V_o denotes the load voltage. With mentioning that the load current I_L is considered as a disturbance, the following linear system can be provided from Eq. (1):

$$\begin{aligned} \dot{x}(t) &= Ax(t) + Bw(t) + Dd(t) \\ y(t) &= Cx(t) \end{aligned} \tag{2}$$

where $x = \begin{bmatrix} Vo \\ I_t \end{bmatrix}$ is the state variable; V_t is the voltage of the converter; $w = V_t$ is the control input; and $d = \begin{bmatrix} I_L \\ 0 \end{bmatrix}$ is the exogenous input of the controlled variable of the system. In addition, $y(t)$ is the measurable output and we assume that $y = x$. Matrices A, B, D and C in the converter model can be indicated as follows [36]:

$$A = \begin{bmatrix} 0 & \frac{1}{C_t} \\ -\frac{1}{L_t} & -\frac{R_t}{L_t} \end{bmatrix}, B = \begin{bmatrix} 0 \\ \frac{1}{L_t} \end{bmatrix}, C = \begin{bmatrix} 1 & 0 \end{bmatrix}, D = \begin{bmatrix} -\frac{1}{C_t} & 0 \\ 0 & 0 \end{bmatrix} \tag{3}$$

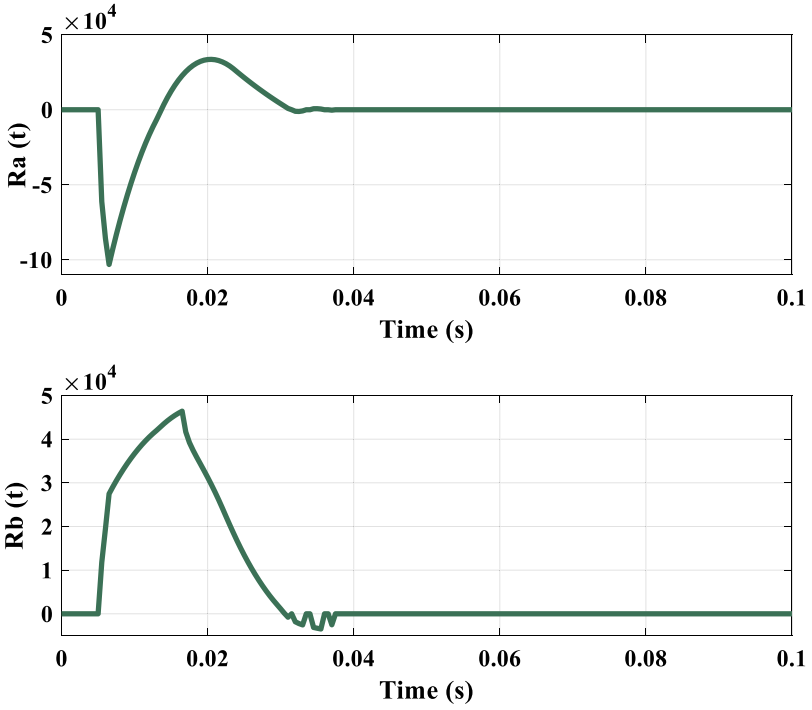

Fig. 7. The outputs of ANN (i.e. $R_a(t)$ and $(R_b(t))$) in study 1.

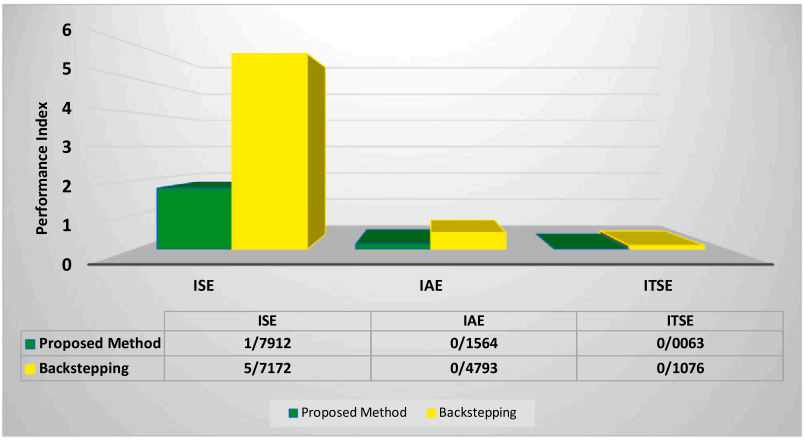

Fig. 8. The performance evaluation graph of controllers in start-up, in study 1.

In addition, the state-space equations of (3) can be extended with regard to the uncertainties in the converter parameters and load current as follows [13]:

$$\begin{aligned}\dot{x}_a &= \frac{1}{C_{tn}}x_b + d_a \\ \dot{x}_b &= -\frac{1}{L_{tn}}x_a - \frac{R_{tn}}{L_{tn}}x_b + \frac{1}{L_{tn}}w + d_b\end{aligned} \tag{4}$$

where $\begin{bmatrix}x_a\\x_b\end{bmatrix} = \begin{bmatrix}Vo\\I_t\end{bmatrix}$; C_{tn}, L_{tn} and R_{tn} are the nominal values of the converter, i.e., capacitance, inductance and resistance parameters, respectively. It is notable that the exact values of the parameters may differ from these nominal values. The perturbation terms d_a and d_b are used to show the modeling errors, aging, uncertainties, and disturbances. The perturbation of the system is simplified by disturbance. We assume that the state variables are finite and the disturbances of d_a and d_b are continuous values and their time derivatives are bounded.

3. Proposed controller design

The proposed controller design method is shown in this section. First, the observer is designed, and then the backstepping controller boundary is discussed based on the stability issue. Finally, the ANN approach is proposed to improve the controller performance.

3.1. Observer and conventional backstepping controller design

I. Disturbance observer design

Based on [31], a disturbance observer for (5) can be obtained by:

$$\begin{aligned}\dot{E}_a &= D_a x_b + \hat{d}_a \\ \dot{E}_b &= f_b(x_a, x_b)D_a x_b + D_b u + \hat{d}_b \\ \hat{d}_a &= \rho_a(x_a - E_a) \\ \hat{d}_b &= \rho_b(x_b - E_b)\end{aligned} \tag{5}$$

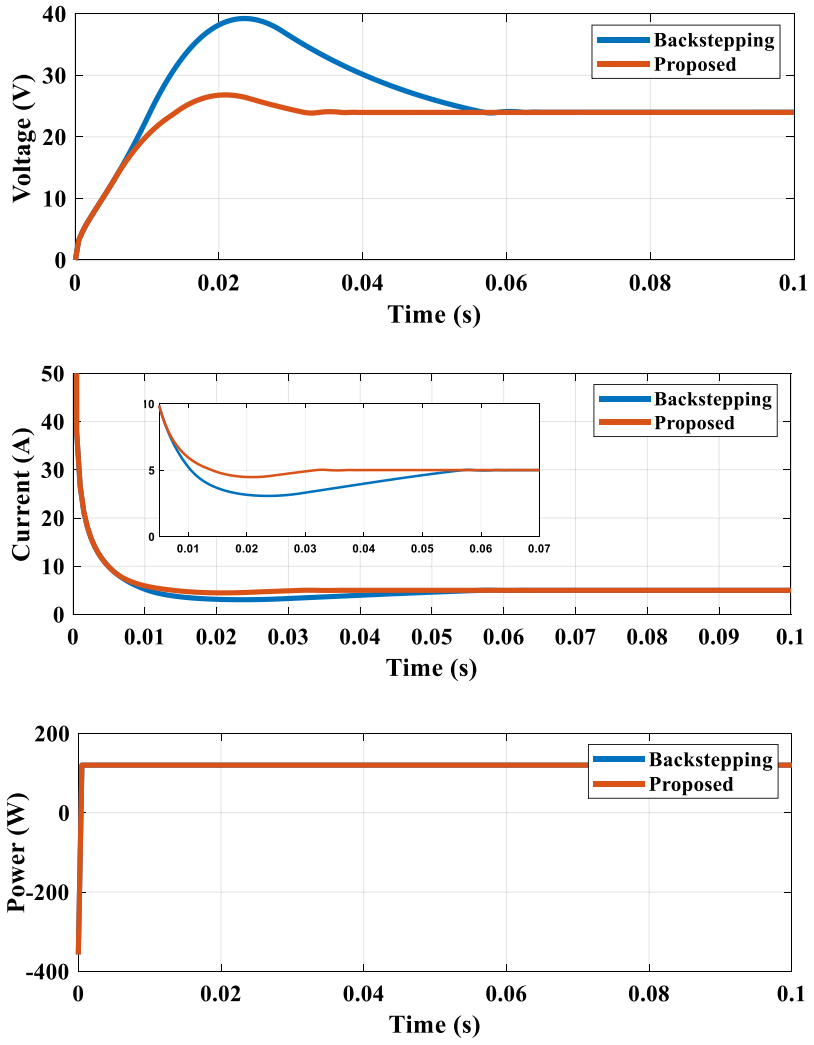

Fig. 9. The simulation results when L increases 5% in study 2.

where ρ_a and ρ_b are the observable positive invariable gains. According to the state-space model in (2) and (3), it can be inferred that:

$$D_a = \frac{1}{C_{tn}}$$
$$f_b(x_a, x_b) = -\frac{1}{L_{tn}}x_a - \frac{R_{tn}}{L_{tn}}x_b \tag{6}$$
$$D_b = \frac{1}{L_{tn}}$$

The disturbances can be shown by:

$$\dot{\hat{d}}_a = \rho_a(\dot{x}_a - \dot{E}_a)$$
$$\dot{\hat{d}}_b = \rho_b(\dot{x}_b - \dot{E}_b) \tag{7}$$

Errors can be estimated by the relationships $e_a = d_a - \hat{d}_a$, $e_b = d_b - \hat{d}_b$ and by deriving the errors and combining with (7). The dynamics of the observer error can be obtained as follows:

$$\dot{e}_a = -\rho_a e_a + \dot{d}_a$$
$$\dot{e}_b = -\rho_b e_b + \dot{d}_b \tag{8}$$

II. Backstepping controller design

The controller intends to adjust the output voltage of converter x_a to the desired value $x_a^\star$ in existence of disturbances, d_a and d_b. The $x_a^\star$ is the reference voltage value. In the following, the proposed controller and the evidence of stability are clarified. A positive definite, continuous, and differentiable Lyapunov function is selected where $q_a = x_a - x_a^\star$.

$$Z_1 = \frac{1}{2}{q_a}^2 + \frac{1}{2}e_a^2 \tag{9}$$

By derivation of Eq. (9), the following can be obtained:

$$\dot{Z}_1 = q_a\dot{q}_a + e_a\dot{e}_a = q_a(D_a x_b + d_a) + e_a(\dot{d}_a - \rho_a e_a) \tag{10}$$

Also, we can write:

$$x_b = x_b - \bar{x}_b + \bar{x}_b = q_b + \bar{x}_b \tag{11}$$

where $q_b = x_b - \bar{x}_b$, and x_b is the virtual control in the backstepping control. The auxiliary function x_b can be formulated as follows:

$$\bar{x}_b = -\frac{1}{D_a}[(R_a + \frac{1}{4T_a})q_a + \hat{d}_a] \tag{12}$$

where $R_a > 0$ and $T_a > 0$. By inserting (11) and (12) into (10):

$$\dot{Z}_1 = -\rho_a e_a^2 + e_a\dot{d}_a + z_a[D_a z_b + d_a - \hat{d}_a - q_a(R_a + \frac{1}{4\rho_a})] = -\rho_a e_a^2 + e_a\dot{d}_a + q_a(D_a q_b + e_a) - q_a^2(k_a + \frac{1}{4T_a}) \tag{13}$$

By applying Young's inequality [37], we can obtain the following equation:

$$q_a e_a \le \frac{1}{4T_a}z_a^2 + T_a e_a^2 \tag{14}$$

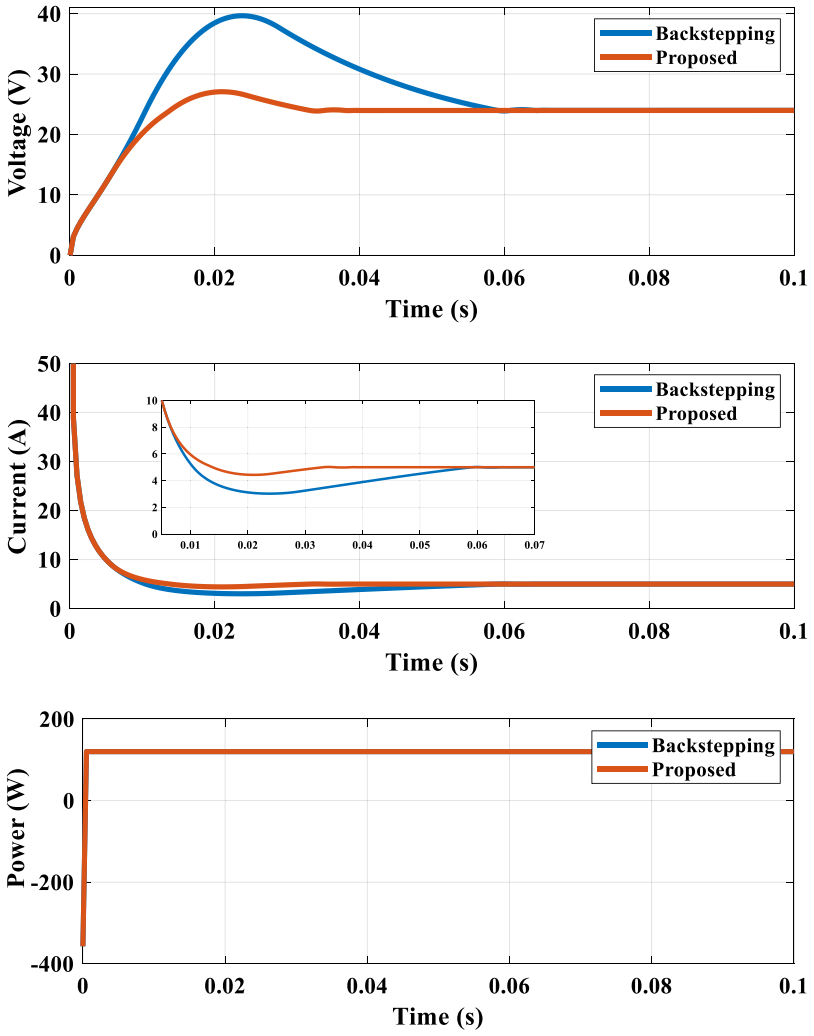

Fig. 10. The simulation results when C increases 5% in study 2.

If we combine (13) and (14), then we will reach the following equation:

$$\begin{aligned}\dot{Z}_1 &\le -\rho_a e_a^2 + e_a \dot{d}_a + D_a q_a q_b + T_a e_a^2 - R_a q_a^2 \\ &\le -e_a^2(\rho_a - T_a) - R_a q_a^2 + D_a q_a q_b + e_a \dot{d}_a\end{aligned} \tag{15}$$

Moreover, a positive definite, continuous, and differentiable Lyapunov function (V) is set as follows:

$$Z = Z_1 + \frac{1}{2}q_b^2 + \frac{1}{2}e_b^2 \tag{16}$$

The time derivative of (16) can be expressed by:

$$\begin{aligned}\dot{Z} \le & -e_a^2\rho_a - T_a - k_a q_a^2 + D_a q_a z_b + e_a \dot{d}_a + z_b[f_b + D_b u \\ & + d_a - \frac{\delta \bar{x}_b}{\delta z_a}(D_a x_b + d_a) - \frac{\delta \bar{x}_b}{\delta \hat{d}_a}\lambda_a e_a] - \rho_b e_b^2 + e_b \dot{d}_b\end{aligned} \tag{17}$$

It is assumed that $A_1 = \frac{\delta \bar{x}_b}{\delta z_a}$, $A_2 = \frac{\delta \bar{x}_b}{\delta \hat{d}_a}$ and $S_b = \frac{1}{4\epsilon_a}(A_1 + A_2\lambda_a)^2$. Therefore, the following can be obtained:

$$\begin{aligned}u &= \frac{1}{D_b}[T_1(D_a x_b + \hat{d}_a) - f_b - \hat{d}_b - D_a q_a - q_b(R_b + \frac{1}{4T_b} + S_b)] \\ &= H_1 x_a + H_2 x_b + H_3 \hat{d}_a + H_4 \hat{d}_b \\ &= (H_1 + \rho_a)x_a + (H_2 + \rho_b)x_b - H_3\rho_a E_a - H_4\rho_b E_b\end{aligned} \tag{18}$$

where $R_b > 0$, $T_b > 0$ and

$$\begin{aligned}H_1 &= L_t n(\frac{1}{L_a} - \frac{1}{C_{tn}} + [-C_{tn}(R_b + \frac{1}{4T_b} + S_b)] * [R_a + \frac{1}{4T_a}]) \\ H_2 &= L_t n[\frac{R_{tn}}{L_{tn}} - (R_a + \frac{1}{4T_a}) - (R_b + \frac{1}{4T_b} + S_b)] \\ H_3 &= -C_{tn}L_{tn}(R_a + \frac{1}{4T_a} + R_b + \frac{1}{4T_b} + S_b) \\ H_4 &= -L_{tn}\end{aligned} \tag{19}$$

If the disturbances fulfill the situation of $\lim_{t\to\infty} \|\dot{d}(t)\|$, and also $d(t) = 0$ at the origin, then the closed-loop system is globally asymptotically stable [11]. The backstepping control method with observer is illustrated in Fig. 3. The notation X^*, in the figure, denotes the reference voltage.

3.2. Proposed intelligent tuning of backstepping weights

The performance of backstepping controller is highly influenced by weighting coefficients, that should be adjusted optimally. The selection of optimal weight based on trial-and-error is a very time-consuming process which needs a massive number of selections and many computer simulations. Evolutionary algorithms are superior to a random trial-and-error search owing to the concepts of fitness pressure, variety, and heredity. If the operating point changes highly, however, ensuring a favorable response is a though task.

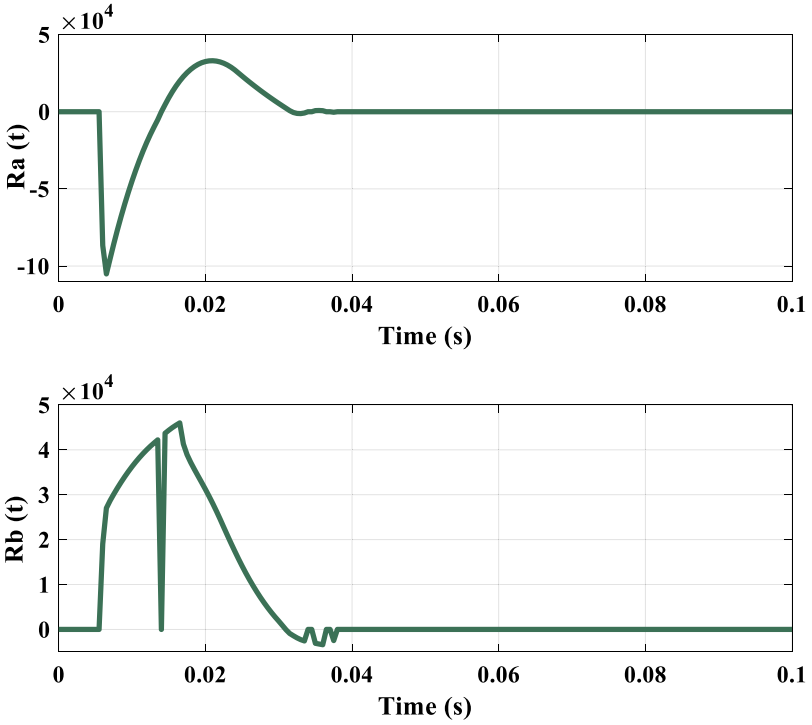

Fig. 11. The outputs of ANN (i.e., $R_a(t)$ and ($R_b(t)$)) when L increases 5% in study 2.

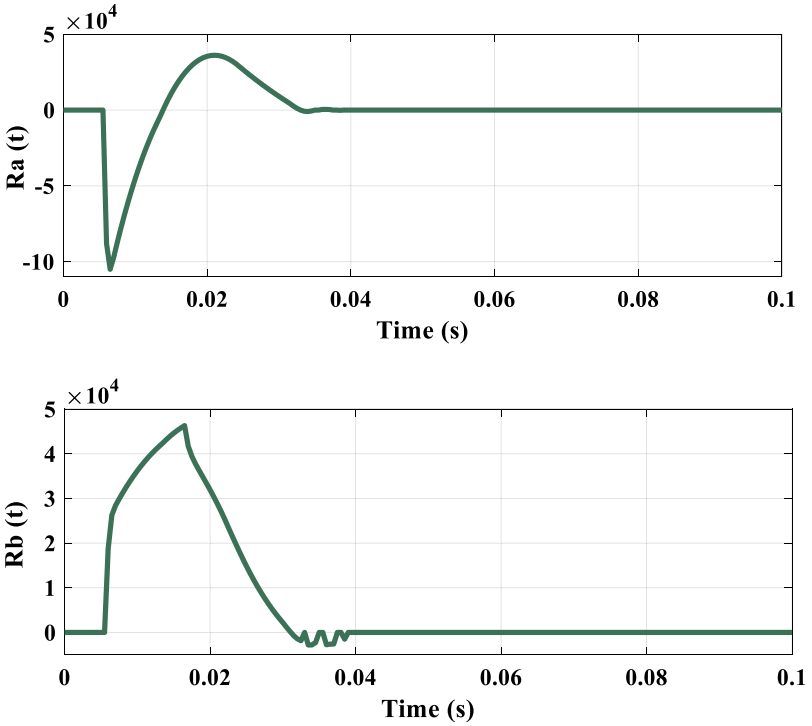

Fig. 12. The outputs of ANN (i.e., $R_a(t)$ and ($R_b(t)$)) when C increases 5% in study 2.

To enhance the ability of the backstepping controller, in this paper, an ANN based approach is proposed for fine tuning of the values of backstepping controller parameters. Intelligent neural network adopts the backstepping controller parameters online. This adaptive feature ensures the robustness of converter under different uncertainties and hence the validity of the proposed method extends to a wider range of operating states. The schematic of the ANN supervisory control for optimal tuning of the backstepping weights is depicted in Fig. 4. It shows $R_a(t) = R_a + dR_a(t)$ and $R_b(t) = R_b + dR_b(t)$ that R_a and R_b are constant. Here, R_a and R_b are constant and equal to values that were constant. In addition, dR_a and dR_b are the ANN outputs. The key functionality of the proposed structure is to minimize the voltage variation as well as its derivative. So, proper set-points are created by ANN and sent to the backstepping controller. Therefore, a safe control operation is achieved that ensures the voltage output stability and robustness.

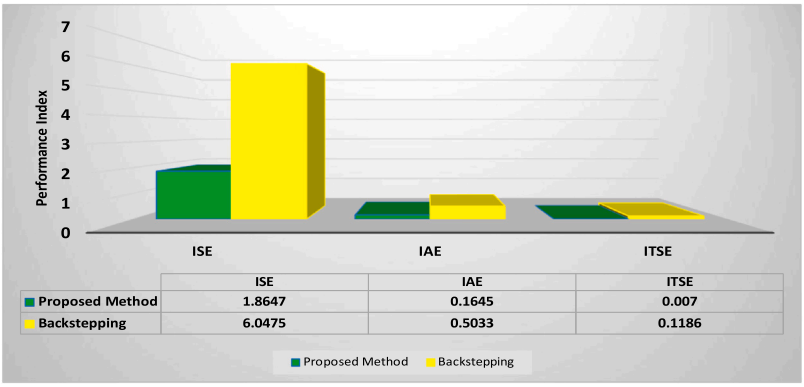

	ISE	IAE	ITSE
Proposed Method	1.8647	0.1645	0.007
Backstepping	6.0475	0.5033	0.1186

Fig. 13. The performance evaluation graph of controllers when C increases 5% in study 2.

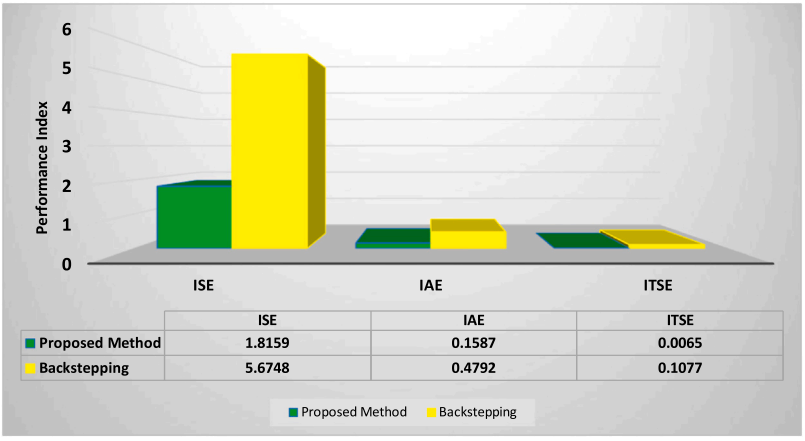

	ISE	IAE	ITSE
Proposed Method	1.8159	0.1587	0.0065
Backstepping	5.6748	0.4792	0.1077

Fig. 14. The performance evaluation graph of controllers when L increases 5% in study 2.

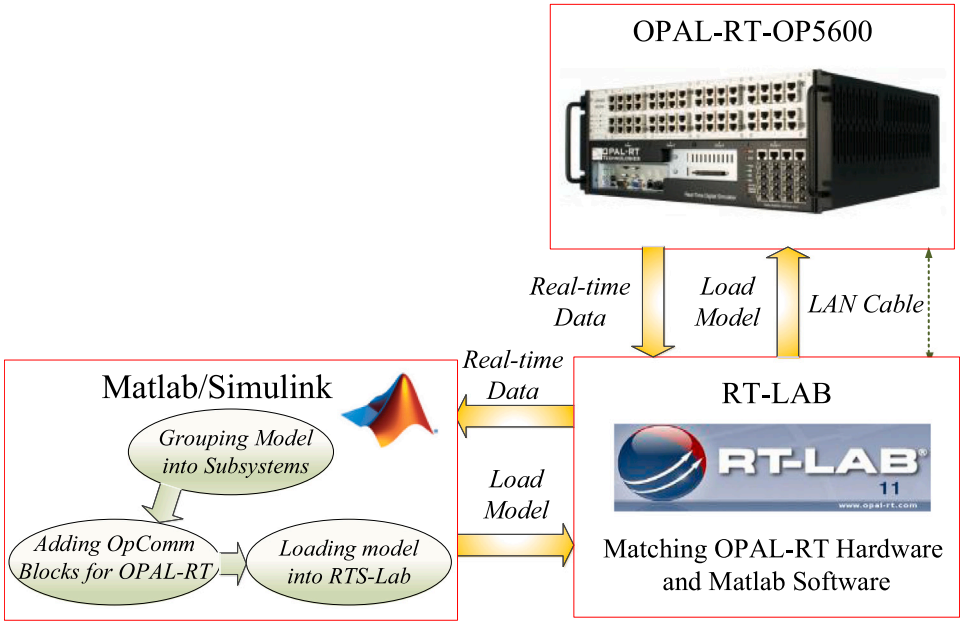

Fig. 15. Real time experimental setup.

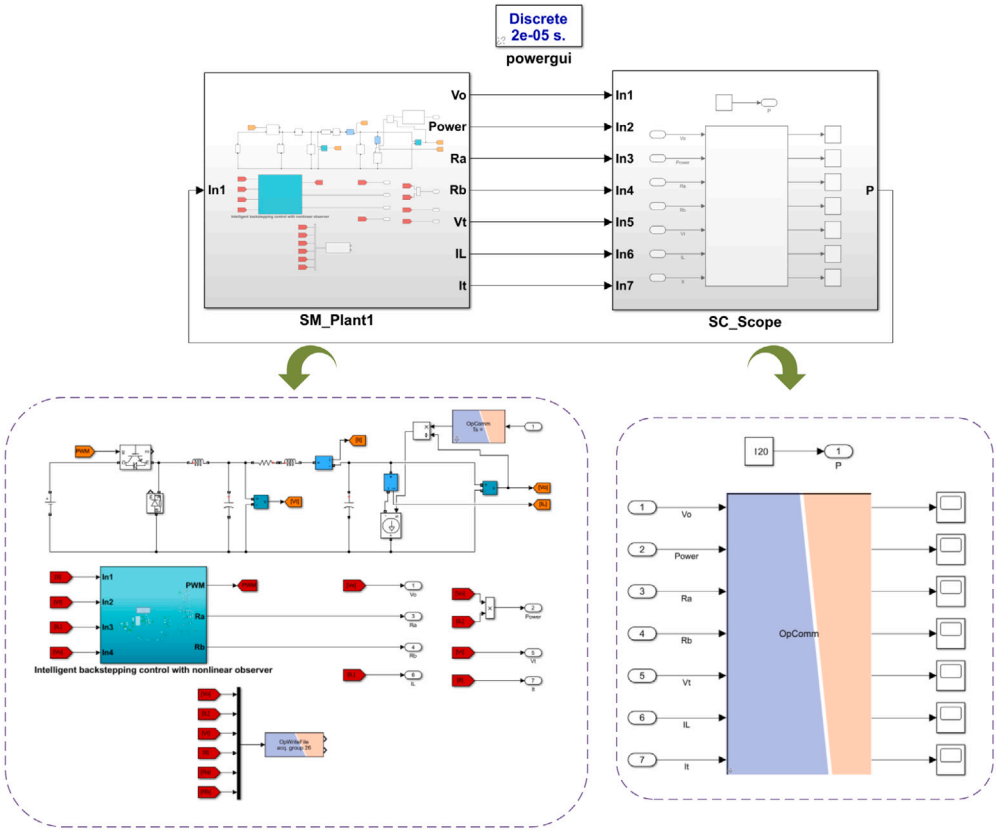

Fig. 16. Matlab and RT-LAB models used in the simulations.

The processing units in an ANN, which are inherently nonlinear, are known as neurons. Each neuron contains three basic elements including weights $w_{ij} = [w_{1j}, w_{2j}, \ldots, w_{nj}]$, an activation function $g(j)$, and a bias parameter φ. Various functions such as sign, tangent sigmoid, and logarithmic sigmoid can be used for the activation function. The input signals indicated by y_i are multiplied by the corresponding weights.

The output of the hidden layer is calculated based on the weighted input and bias as mathematically shown in (20):

$$H_j = g\left(\sum_{i=1}^{n} w_{ij} y_i + \varphi\right) \qquad j = 1, 2, \ldots, L \tag{20}$$

where L is the number of nodes in the hidden layer.

Then, the output of the output layer (the outputs are the backstepping weights) can be obtained as follows:

$$O_c = \sum_{j=1}^{L} H_j w_{jc} + \varphi \qquad c = 1, 2, \ldots, m \tag{21}$$

where m is the number of nodes in the output layer.

The learning procedure deals with the minimization of mean squared error as follows:

$$E = \frac{1}{2} \sum_{r=1}^{N} \left(V_o - X^*\right)^2 \tag{22}$$

where N is the number of samples.

The weights of the ANN are updated based on supervised feedback approach in which the back-propagation algorithm is used for the learning procedure of the ANN coordinator [38].

The calculated error value in (22) is employed to update the ANN weights as follows:

$$w_{ij}(k+1) = w_{ij}(k) + \eta \delta y$$
$$i = 1, 2, \ldots, n \qquad j = 1, 2, \ldots, L \tag{23}$$

$$w_{jc}(k+1) = w_{jc}(k) + \eta H_j E_c$$
$$j = 1, 2, \ldots, L \qquad c = 1, 2, \ldots, m \tag{24}$$

It is to be noted that in Fig. 5, W_1 represents the weight vector for the hidden layer whereas W_2 is similarly deployed for the output. E_c denotes the error signals including the voltage variation and its derivative.

In the design process of the proposed ANN based fine tuner structure, it is considered that the input layer of ANN has 10 linear neurons, and there are 20 nonlinear neurons for the hidden layer. The number of neurons in input/hidden layers are determined through a trial and error process. Moreover, the output layer of ANN must contain analogous number of neurons to the control variables. Since the control variables are the weights of the backstepping controller, two linear neurons are considered in the output layer.

4. Simulation results

In this section, the intelligent backstepping controller based on the nonlinear observer is evaluated to stabilize the CPL buck converter. Table 1 summarizes the parameters of the studied system. The following studies have been performed to evaluate the performance of the proposed control method for the buck dc–dc converter. The transient outputs of the proposed system are compared with the backstepping controller with the nonlinear observer in start-up condition and reference voltage variation, as well as to confirm the robustness of the proposed method against the uncertainty of the parameters. In uncertainty analysis, some of the converter parameters (i.e., L and C) are increased by 5% compared to their nominal values. The corresponding controller parameters, T_a, T_b, ρ_a and ρ_b are chosen as 2, 0.5, 8 and 0.9, respectively. In conventional backstepping controller, R_a and R_b are constant and they are set as 10 000 and 20 000, respectively. While, in the proposed method, these two parameters are regulated by neural

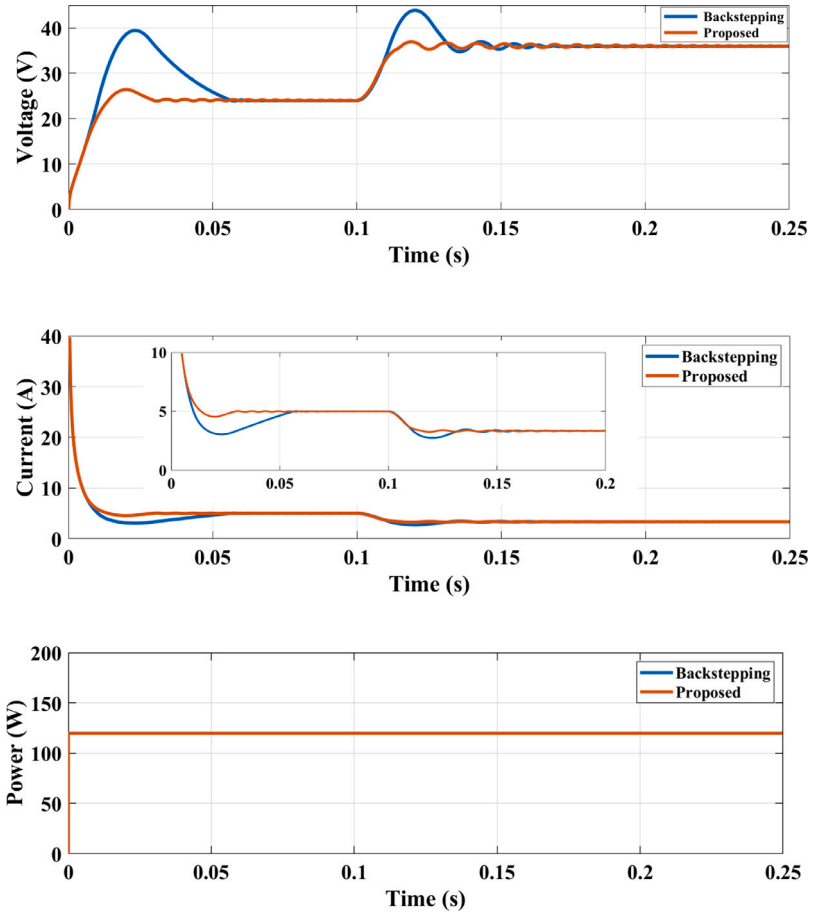

Fig. 17. The OPAL-RT results when reference voltage changes.

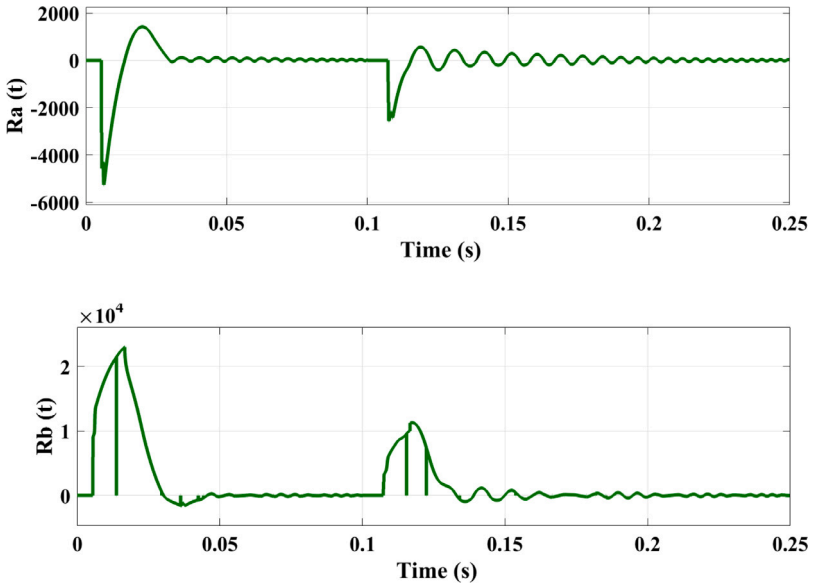

Fig. 18. The outputs of ANN (i.e., $R_a(t)$ and ($R_b(t)$)) when reference voltage changes.

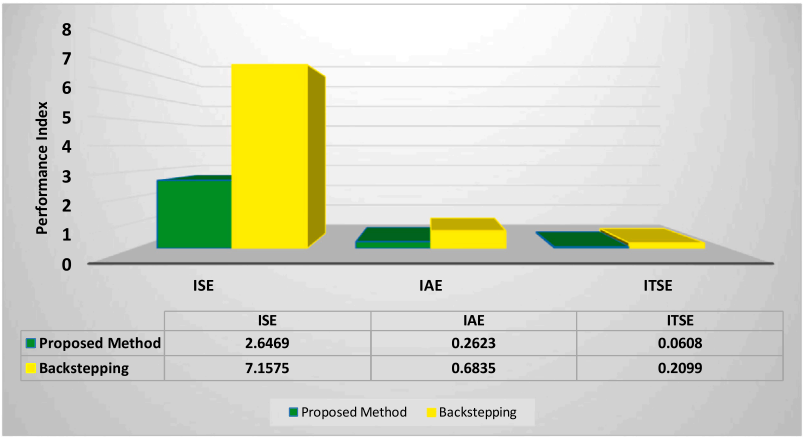

Fig. 19. The performance evaluation graph of controllers when reference voltage changes.

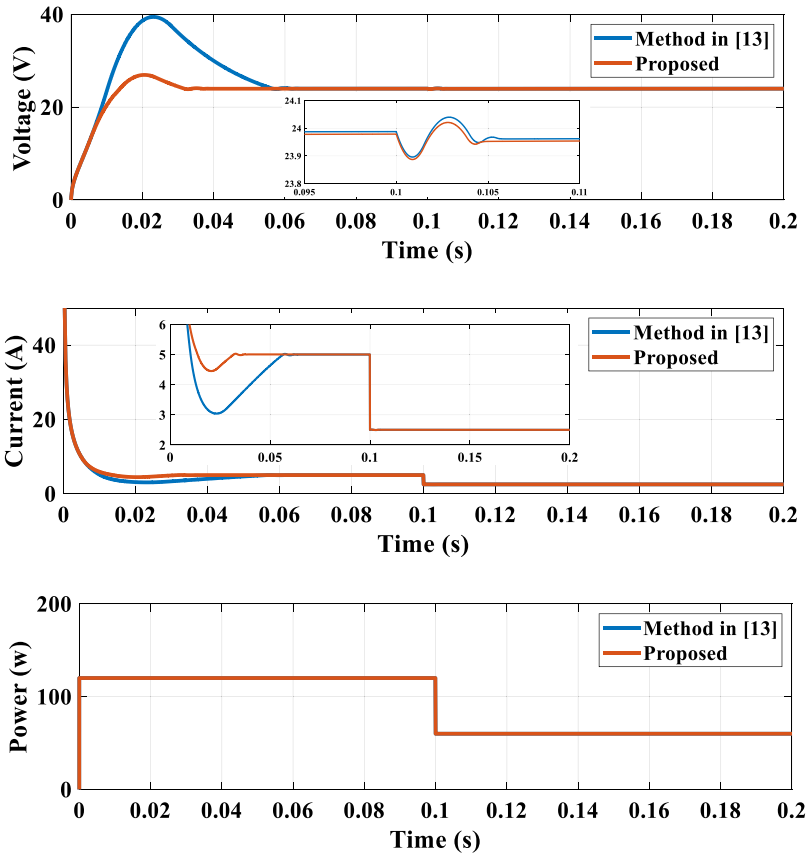

Fig. 20. The OPAL-RT results when CPL changes.

network. It is worth mentioning that $R_a(t)$ and $R_b(t)$, as mentioned in 3.1, must be positive.

4.1. Study 1

In the first study, the start-up condition has been evaluated during the change of output voltage to 24 V. For this study, the response of the proposed controller and backstepping controller with observer are shown in Fig. 3. The output voltage of the backstepping control method with the observer and the proposed method can be seen in Fig. 6. During the start-up, the backstepping with observer generates a large

Table 1
Parameters of the test system used in simulations.

Parameter	Symbol	Value
Input voltage	E	80 V
Reference voltage	X^*	24 V
Filter capacitance	C_t	220 μF
Filter inductance	L_t	450 μH
Filter resistance	R_t	0.3 Ω
CPL	P_{CPL}	120 W

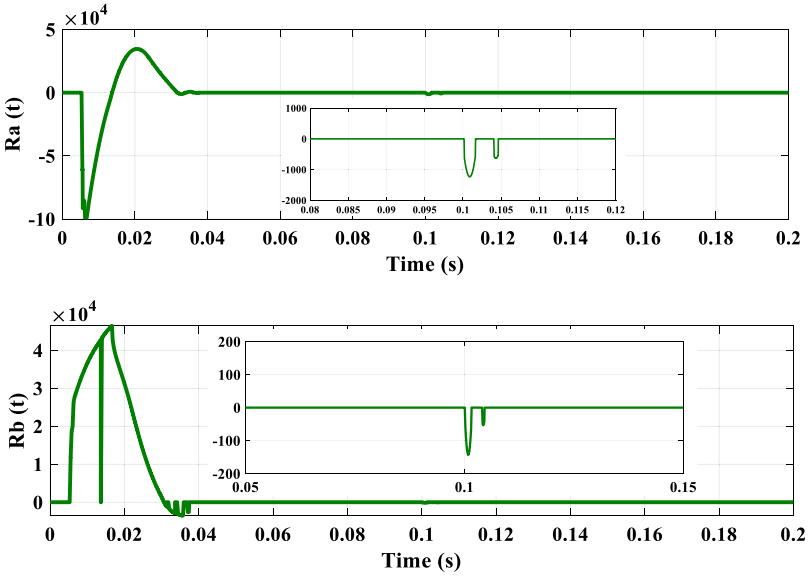

Fig. 21. The outputs of ANN (i.e., $R_a(t)$ and ($R_b(t)$)) when CPL changes.

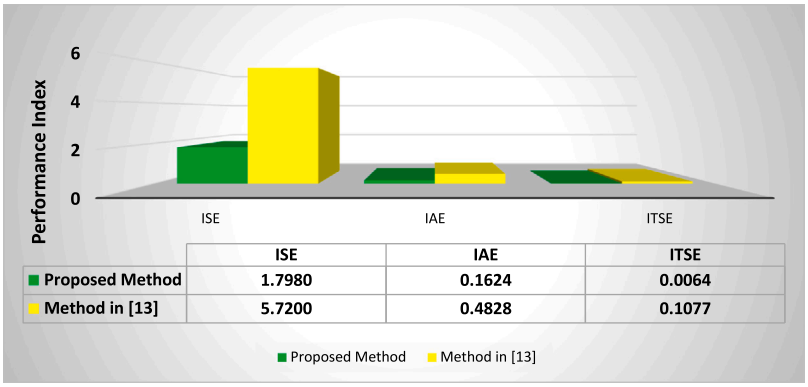

	ISE	IAE	ITSE
Proposed Method	1.7980	0.1624	0.0064
Method in [13]	5.7200	0.4828	0.1077

Fig. 22. The performance evaluation graph of controllers when CPL changes.

voltage overshoot about 40 V and settling time of 0.06 s, to reach the 24 v. While the proposed method decreases the overshoot and settling time to 26 V and 0.034 s, respectively. As illustrated in the figure, the proposed method diminishes the voltage overshoot and settling time considerably compared to the backstepping with observer method. Similar discussion is true about the current where the backstepping with observer control produces an undershoot of 40% in output current, converges to 6 A in 0.06 s and has a large peak compared to the proposed method, in which the time to achieve desired amps is 0.035 s. Variations of $R_a(t)$ and $R_b(t)$ parameters, resulting from ANN, are shown in Fig. 7. As it was mentioned, these values have been added to the constant values of R_a and R_b to improve the robustness of the controller.

In addition, in order to evaluate the performance of the proposed method from different aspects, some of the performance specifications of the buck converter are given in the following. The sum of the integral time square error (ITSE), integral absolute error (IAE), and integral square error (MAE) for the study 1 is shown in Fig. 8. As can be seen, the graph indicates the acceptable performance of the proposed control method in this study compared to the backstepping method.

4.2. Study 2

In this section, robustness of the proposed control scheme against the plant parametric uncertainty is examined. To investigate this issue, two parameters of the converter, i.e. L and C, are increased 5% from their nominal values.

The output voltage, current and power when the L increases are illustrated in Fig. 9. It is demonstrated that the voltage and current deviations in stable time are less than 15% and 1.5%, respectively, while they are 0.625 and 0.4 in the backstepping with the observer controller. Fig. 10, corresponding to change of C when 5% increases, shows that the proposed method yields relatively smaller peak undershoot in current and overshoot in voltage, along with fast settlement.

The variations of $R_a(t)$ and $R_b(t)$ in this study are available in Figs. 11 and 12. Here, like the previous study, the ITSE, IAE and MAE indices for controllers in uncertain situations, when C and L are increased 5%, can be seen in Figs. 13 and 14. The results in the studies 1 and 2 demonstrate the suitable performance of the proposed method in start-up and converter parameters changes.

4.3. Study 3

In this study, the buck dc–dc converter with the proposed control method is implemented in the real-time simulator, OPAL-RT-OP5600, to verify its applicability and effectiveness in real-time. Fig. 15 shows the broad configuration of the experimental setup. Fig. 16 illustrates the Matlab and RT-LAB models used in this work. In this section, two real-time scenarios for the evaluation of the proposed control strategy are utilized. In the first scenario, an ideal CPL and a change

in the reference voltage are assumed. In response to the CPL being constant and the reference voltage changing, the output voltage in the proposed controller method tracks the reference voltage, while the voltage response in the conventional backstepping with observer method suddenly fluctuates larger at $t = 0.1$ s. The power of CPL is constant and equal to 120 w in real-time simulation whereas the reference voltage is 24 V for $t \in [0, 0.1]$ sec and it increases to 36 for $t \in [0.1, 0.25]$ sec. The output voltage of the CPL is shown in Fig. 17. As can be seen, when the reference voltage changes to 36 V, the proposed method can settle the voltage faster and smoother than the backstepping with observer controller. The overshoot in backstepping with observer is 26 V while the overshoot in the proposed method is 39 V. The current of CPL which was controlled by the proposed method settles faster and better than the current of CPL which was controlled by the backstepping with observer. Therefore, the proposed controller can recover faster and better CPL's voltage and current. The output of ANN in this study can be found in Fig. 18. Also, some of the converter performance indices for this study like the previous studies, in order to show better performance of the proposed method, can be found in Fig. 19. Another real-time scenario for the proposed control scheme evaluation is investigated, which involves a dynamic change in the CPL. For this end, a power decrease of 60 W at t = 0.1 s is assumed. The output voltage, current and power are shown in Fig. 20. The results are compared to a traditional backstepping controller reported in [13]. As the results imply, the proposed control method, yields less voltage overshoot and current undershoot than the method in [13]. The figure also suggests that, by making use of the proposed control scheme, the voltage fluctuation during a noticeable change in load is less than 0.2 V (i.e., less than 0.8% of the desired output voltage) which is an ideal value. The ANN outputs can be found in Fig. 21, and the converter performance indices when the CPL changes compared to the method in [13] are given in Fig. 22. The results, as the previous scenarios, indicate the superior performance of the proposed method during the execution of this scenario.

5. Conclution

This paper proposed an intelligent adaptive backstepping control based on an ANN to regulate the output voltage of dc/dc converter feeding a CPL. The parameters of the controller were estimated by the proposed ANN controller. The controller was designed according to the stability issue and transient performance. The proposed control method was investigated for the response of start-up, reference voltage variations, uncertainties and load variation of converter parameters' situations. Thus, fast dynamic response of the simulation results ensured the accurate voltage tracking. Comparing the proposed control with the conventional backstepping controller indicated better performance of the proposed method. This controller can be investigated for other converters and in large-scale microgrids as a future work.

CRediT authorship contribution statement

Hoda Sorouri: Writing – original draft, Software, Visualization. **Mostafa Sedighizadeh:** Validation, Writing – review & editing. **Arman Oshnoei:** Software, Writing – review & editing, Methodology. **Rahmat Khezri:** Conceptualization, Methodology, Writing – review & editing.

Declaration of competing interest

The authors declare that they have no known competing financial interests or personal relationships that could have appeared to influence the work reported in this paper.

References

[1] Emadi A, Khaligh A, Rivetta CH, Williamson GA. Constant power loads and negative impedance instability in automotive systems: Definition, modeling, stability, and control of power electronic converters and motor drives. IEEE Trans Veh Technol 2006;55(4):1112–25.

[2] Doerry N. Next generation integrated power systems NGIPS technology development roadmap. 2007, p. 120, November 2007.

[3] Wu M, Lu DDC. A novel stabilization method of LC input filter with constant power loads without load performance compromise in DC microgrids. IEEE Trans Ind Electron 2015;62(7):4552–62.

[4] Dragicevic T, Lu X, Vasquez JC, Guerrero JM. DC microgrids - Part I: A review of control strategies and stabilization techniques. IEEE Trans Power Electron 2016;31(7):4876–91.

[5] Xiao J, Wang P, Setyawan L, Xu Q. Multi-level energy management system for real-time scheduling of DC microgrids with multiple slack terminals. IEEE Trans Energy Convers 2016;31(1):392–400.

[6] Chan CY. A nonlinear control for dc-dc power converters. IEEE Trans Power Electron 2007;22(1):216–22.

[7] Sundareswaran K, Devi V, Sankar S, Nayak PSR, Peddapati S. Feedback controller design for a boost converter through evolutionary algorithms. IET Power Electron 2014;7(4):903–13.

[8] Vijay V, Yadav SK, Adhikari B, Seshadri H, Fulwani DK. Systems thinking approach for social problems. In: Proceedings of 37th national systems conference, December 2013. Lecture notes in electrical engineering, vol. 327, 2015, p. i–iv.

[9] Bottrell N, Prodanovic M, Green TC. Dynamic stability of a microgrid with an active load. IEEE Trans Power Electron 2013;28(11):5107–19.

[10] Meng L, Shafiee Q, Trecate GF, Karimi H, Fulwani D, Lu X, Guerrero JM. Review on control of DC microgrids and multiple microgrid clusters. IEEE J Emerg Sel Top Power Electron 2017;5(3):928–48.

[11] Amiri H, Markadeh GA, Dehkordi NM. Voltage control and load sharing in a DC islanded microgrid based on disturbance observer. In: ICEE 2019-27th Iranian conference on electrical engineering. 2019, p. 825–30.

[12] Grigore V, Hatonen J, Kyyra J, Suntio T. Dynamics of a buck converter with a constant power load. In: PESC record - IEEE annual power electronics specialists conference, 1(June). 1998, p. 72–8.

[13] Amiri H, Markadeh GRA, Dehkordi NM, Blaabjerg F. Fully decentralized robust backstepping voltage control of photovoltaic systems for DC islanded microgrids based on disturbance observer method. ISA Trans 2020;101:471–81.

[14] Cai D, Shi D, Chen J. Electrical power and energy systems probabilistic load flow with correlated input random variables using uniform design sampling. Int J Electr Power Energy Syst 2014;63:105–12.

[15] Amiri H, Markadeh GA, Dehkordi NM. Voltage control in a DC islanded microgrid based on nonlinear disturbance observer with CPLs. J Energy Storage 2020;29(1):1–10.

[16] Herrera L, Zhang W, Wang J. Stability analysis and controller design of DC microgrids with constant power loads. IEEE Trans Smart Grid 2017;8(2):881–8.

[17] Zhao Y, Qiao W, Ha D. A sliding-mode duty-ratio controller for DC/DC buck converters with constant power loads. IEEE Trans Ind Appl 2014;50(2):1448–58.

[18] Solsona JA, Jorge SG, Busada CA. Nonlinear control of a buck converter which feeds a constant power load. IEEE Trans Power Electron 2015;30(12):7193–201.

[19] Qian Z, Abdel-Rahman O, Al-Atrash H, Batarseh I. Modeling and control of three-port DC/DC converter interface for satellite applications. IEEE Trans Power Electron 2010;25(3):637–49.

[20] Tahim APN, Pagano DJ, Ponce E. Nonlinear control of dc-dc bidirectional converters in stand-alone dc Microgrids. In: Proceedings of the IEEE conference on decision and control. 2012, pp. 3068–73.

[21] Lin X, Liu J, Liu F, Liu Z, Gao Y, Sun G. Fractional-order sliding mode approach of buck converters with mismatched disturbances. IEEE Trans Circuits Syst 2021;68(9):3890–900.

[22] Liu J, Shen X, Alcaide A, Yin Y, Leon J, Vazquez S, Wu L, Franquelo L. Sliding mode control of grid-connected NPC converters via high-gain observer. IEEE Trans Ind Electron 2021.

[23] Liu J, Laghrouche S, Wack M. Observer-based higher order sliding mode control of power factor in three-phase AC/DC converter for hybrid electric vehicle applications. Internat J Control 2014;87(6):1117–30.

[24] Yin Y, Liu J, Sanchez J, Wu L, Vazuez S, Leon J, Franquelo L. Observer-based adaptive sliding mode control of NPC converters: An RBF neural network approach. IEEE Trans Power Electron 2019;34(4):3831–41.

[25] Zhou W, Ye X. Adaptive control of parallel DC-dc buck converters with uncertain parameters. In: 2012 12th international conference on control, automation, robotics and vision, ICARCV 2012, 2012(December). 2012, p. 737–40.

[26] Zhou W, Liu B Bin. Analysis and design of DC-DC buck converter with nonlinear adaptive control. In: ICCSE 2012 - Proceedings of 2012 7th international conference on computer science and education, Iccse. 2012, p. 736–1038.

[27] Giri F, Bai EW. Lecture notes in control and information sciences: Preface. Lecture notes in control and information sciences, vol. 404, 2010.

[28] Ashabani SM, Mohamed YARI. A flexible control strategy for grid-connected and islanded microgrids with enhanced stability using nonlinear microgrid stabilizer. IEEE Trans Smart Grid 2012;3(3):1291–301.

[29] Lee TS, Chen ML. Applied nonlinear control with adaptive backstepping technique for a three-phase AC/DC boost converter. In: IECON proceedings (Industrial electronics conference). 2008, p. 567–71.
[30] El Fadil H, Giri F. Backstepping based control of PWM DC-DC boost power converters. In: IEEE international symposium on industrial electronics. 2007, p. 395–400.
[31] Chen WH, Yang J, Guo L, Li S. Disturbance-observer-based control and related methods - An overview. IEEE Trans Ind Electron 2016;63(2):1083–95.
[32] Zhang C, Wang J, Li S, Wu B, Qian C. Robust control for PWM-based DC-DC buck power converters with uncertainty via sampled-data output feedback. IEEE Trans Power Electron 2015;30(1):504–15.
[33] Qian C, Member S, Lin W, Member S. QL01-IEEETAC.pdf. 2001;46(7):1061–79.
[34] Polyakov A, Efimov D, Perruquetti W. Robust stabilization of MIMO systems in finite/fixed time. Internat J Robust Nonlinear Control 2015;23.
[35] Tucci M, Riverso S, Vasquez JC, Guerrero JM, Ferrari-Trecate G. Voltage control of DC islanded microgrids: A decentralized scalable approach. In: Proceedings of the IEEE conference on decision and control, 54rd IEEE conference on decision and control, CDC 2015(Lmi). 2015; p. 3149–54.
[36] Diaz JB, Metcalf FT. An analytic proof of Young's inequality. Amer Math Monthly 1970;77(6):603–9.
[37] Bismarck-Nasr MN. Nonlinear systems. In: Structural dynamics in aeronautical engineering. 1999, p. 119–38.
[38] Khezri R, Oshnoei A, Yazdani A, Mahmoudi A. Intelligent coordinators for automatic voltage regulator and power system stabiliser in a multi-machine power system. IET Gener Transm Distrib 2020;14(23):5480–90.